

AD-A257 766



PL-TR-92-2094

2

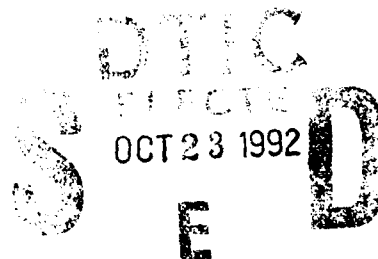
MEASUREMENTS OF F-REGION DRIFT VELOCITIES AT THE DUSK SECTOR MID-LATITUDE TROUGH

**James L. Scali
Bodo W. Reinisch**

**University of Massachusetts, Lowell
Center for Atmospheric Research
450 Aiken Street
Lowell, MA 01854**

March 1992

Scientific Report No. 1



APPROVED FOR PUBLIC RELEASE; DISTRIBUTION UNLIMITED




**PHILLIPS LABORATORY
Directorate of Geophysics
AIR FORCE SYSTEMS COMMAND
HANSCOM AIR FORCE BASE, MA 01731-5000**


92-27742



This technical report has been reviewed and is approved for publication.


JURGEN BUCHAU
Contract Manager


JOHN E. RASMUSSEN, Chief
Ionospheric Application Branch


WILLIAM K. VICKERY, Director
Ionospheric Effects Division

This document has been reviewed by the ESD Public Affairs Office (PA) and is releasable to the National Technical Information Service (NTIS).

Qualified requestors may obtain additional copies from the Defense Technical Information Center. All others should apply to the National Technical Information Service.

If your address has changed, or if you wish to be removed from the mailing list, or if the addressee is no longer employed by your organization, please notify PL/TSI, Hanscom AFB, MA 01731-5000. This will assist us in maintaining a current mailing list.

Do not return copies of this report unless contractual obligations or notices on a specific document requires that it be returned.

REPORT DOCUMENTATION PAGE

Form Approved
OMB No 0704-0188

Public reporting burden for this collection of information is estimated to average 1 hour per response, including the time for reviewing instructions, searching existing data sources, gathering and maintaining the data needed, and completing and reviewing the collection of information. Send comments regarding this burden estimate or any other aspect of this collection of information, including suggestions for reducing this burden, to Washington Headquarters Services, Directorate for Information Operations and Reports, 1215 Jefferson Davis Highway, Suite 1204, Arlington, VA 22202-4302, and to the Office of Management and Budget, Paperwork Reduction Project (0704-0188), Washington, DC 20503.

1. AGENCY USE ONLY (Leave blank) 2. REPORT DATE
March 1992 3. REPORT TYPE AND DATES COVERED
Scientific No. 1

4. TITLE AND SUBTITLE
Measurements of F-Region Drift Velocities at
the Dusk Sector Mid-Latitude Trough 5. FUNDING NUMBERS
PE 62101F
PR 4643
TA 08
WU AU
Contract Number
F19628-90-K-0005

6. AUTHOR(S)
James L. Scali and Bodo W. Reinisch 7. PERFORMING ORGANIZATION NAME(S) AND ADDRESS(ES)
University of Massachusetts Lowell
Center for Atmospheric Research
450 Aiken Street
Lowell, MA 01854 8. PERFORMING ORGANIZATION
REPORT NUMBER

9. SPONSORING/MONITORING AGENCY NAME(S) AND ADDRESS(ES)
Phillips Laboratory
Hanscom AFB, MA 01731-5000 10. SPONSORING/MONITORING
AGENCY REPORT NUMBER
PL-TR-92-2094
Contract Manager: Jurgen Buchau/GPIA

11. SUPPLEMENTARY NOTES

12a. DISTRIBUTION / AVAILABILITY STATEMENT
Approved for public release;
distribution unlimited 12b. DISTRIBUTION CODE

13. ABSTRACT (Maximum 200 words)
Drift velocities measured at the high latitude Digisonde stations
Goose Bay, Argentina, and Millstone Hill are used to investigate
the formation of mid-latitude troughs in the dusk sector. The
observations show the existence of westward drift velocities of
magnitudes comparable to the velocity of the earth's rotation
during trough formation. These drifts are part of the two cell
convection pattern as implied by the stagnation theory of trough
formation.

14. SUBJECT TERMS
Trough, Drift, Stagnation Region, Horizontal
Velocity, Vertical Velocity, Azimuth 15. NUMBER OF PAGES
38 16. PRICE CODE

17. SECURITY CLASSIFICATION
OF REPORT
Unclassified 18. SECURITY CLASSIFICATION
OF THIS PAGE
Unclassified 19. SECURITY CLASSIFICATION
OF ABSTRACT
Unclassified 20. LIMITATION OF ABSTRACT
SAR

TABLE OF CONTENTS

	Page
1.0 INTRODUCTION	1
2.0 DIGISONDE DATA AND ANALYSIS METHOD.....	3
3.0 SYSTEMATIC TROUGH DETECTION	6
4.0 DRIFT VELOCITIES IN THE DUSK SECTOR.....	16
5.0 CONCLUSION.....	28
6.0 REFERENCES	29

Acquisition For	
ENTIS - C3301	<input checked="" type="checkbox"/>
ENTIS - 1745	<input checked="" type="checkbox"/>
Unidentified	<input type="checkbox"/>
Unidentified	<input type="checkbox"/>
By	
Dr. [unclear]	
Availability Codes	
Dist	Availability for Special
A-1	

LIST OF ILLUSTRATIONS

Figure No.		Page
1	The diurnal variation of V_z , V_h , f_oF_2 and h_mF_2 observed at Millstone Hill on 25 January 1991.....	5
2	Diurnal variations in f_oF_2 and h_mF_2 averaged over the three most geomagnetically quiet days during the months of (a) January, (b) February and (c) March 1990.....	7
3	Contour plots for P_{hf} for March 1990 at Millstone Hill.....	8
4	Contour plots for P_{hf} for March 1990 at Argentina.....	9
5	Contour plots for P_{hf} for March 1990 at Goose Bay. (a) Contours calculated using the 3-day average quiet days results recorded at Goose Bay, (b) Contours calculated using the 3-day average quiet days results recorded at Millstone Hill.....	10
6	Ratio P_{hf} plotted with respect to sum of K_p for 41 days when troughs were detected at Millstone Hill.....	13
7	Ratio P_{hf} plotted with respect to sum of K_p for 44 days when troughs were detected at Argentina.....	14
8	Ratio P_{hf} plotted with respect to sum of K_p for 55 days when troughs were detected at Goose Bay.....	15
9	High latitude two cell convection pattern. (a) Represents the non rotating frame of reference while (b) corotation has been added. The flow stagnation point is located around 22 CGLT. Reproduced from Spiro et. al., [1978].....	17

LIST OF ILLUSTRATIONS (Continued)

Figure No.		Page
10	Polar plots for (1) foF2, (b) hmF2, (c) Vh and (d) Vz, observed at Millstone Hill on day 047 1990.....	19
11	Polar plot of horizontal velocity vectors observed at Millstone Hill on days (a) 103 and (b) 104, 1990	20
12	Polar plots for (a) foF2, (b) hmF2, (c) Vh and (d) Vz, observed at Argentina on day 38, 1990.....	22
13	Polar plots for (a) foF2, (b) hmF2, (c) Vh and (d) Vz, observed at Goose Bay on day 138, 1990	23
14	Statistical analysis of Az, Vh and Vz measured over 41 days when troughs were detected at Millstone Hill during January -June, 1990 (a) median of Az, (b) mean of Vh and (c) mean of Vz 	24
15	Statistical analysis of Az, Vh and Vz measured over 44 days when troughs were detected at Argentina during January - June, 1990, (a) median of Az, (b) mean of Vh and (c) mean of Vz 	26
16	Statistical analysis of Az, Vh and Vz measured over 55 days when troughs were detected at Goose Bay during January - June, 1990, (a) median of Az, (b) mean of Vh and (c) mean of Vz 	27

1.0 INTRODUCTION

One of the most prominent features of the nightside electron density distribution is a well defined ionization-depleted sector in the F-region known as the mid-latitude trough. In general, the mid-latitude trough is geomagnetically orientated along a circumpolar region at an L-shell value of approximately 4. Being originally considered as the boundary region between the mid-latitude and polar ionosphere, it occurs both in the northern and southern hemispheres.

The first observations and identification of a depletion zone in electron density measurements at F-region heights in the auroral zone was made by Muldrew [1965] and Sharp [1966]. It was Muldrew [1965] who gave it the name "main trough", so as to distinguish it from other temporary high-latitude troughs. However other names have been used in the literature to describe the same phenomenon. In the ensuing discussions the terms "mid-latitude" and "main" trough will be taken to mean the depletion of F-region electron densities at sub-auroral latitudes, which are mostly seen as a nocturnal feature.

Extensive investigations on the characteristics of the main trough have been carried out [Moffet and Quegan, 1983]. From these observations we extracted the following list of main features of the trough:

- a) The main trough is generally a nightside phenomenon, although it has been observed in the pre-dusk, dawn and noon time sectors, especially at latitudes above $\approx 70^\circ$ MLAT in winter months (Whalen, 1992). Frequently observed after sunset, it extends from the dusk to the dawn sector.
- b) It is more pronounced during autumn and winter months and less evident in spring and summer. In summer the trough only occurs near local midnight.
- c) The trough center under very quiet conditions is located near 65° corrected geomagnetic latitude, with a width of approximately 10° at the maximum of the F-region peak [Mendillo & Chacko, 1977; Evans et al., 1983].

- d) The poleward edge of the trough generally displays a latitudinal extent of 1.5° in comparison to the 7° observed for the equatorial edge [Mendillo and Chacko, 1977]. The equatorial edge of the auroral oval is usually regarded as the poleward edge of the main trough [Liszka and Turunen, 1970].
- e) From a ground-based station the latitude of the trough appears to decrease throughout the night. Since the apparent movement at magnetic quiet times is purely attributed to the rotation of the earth, a movement back towards higher latitudes is observed in the dawn sector.
- f) The position of the main trough primarily depends on magnetic activity and local time. For example, during periods of increased magnetic activity the trough moves to lower latitudes.

From statistical analysis of the main trough position empirical formulas were derived for the location of the center of the main trough [Rycroft and Thomas, 1970; Rycroft and Burnell, 1970; Halcrow and Nisbet, 1977]. Rycroft and Thomas, [1970] concluded that the center of the plasma pause at 1000 km altitude and the center of the main trough both lie on the same geomagnetic field line

Two of the most promising theories to explain the formation of the nocturnal trough are the so called "stagnation theory" [Knudsen 1974; Knudsen et al., 1977; Spiro et al., 1978] and the "enhanced recombination theory" [Banks et al., 1974; Schunk et al., 1975]. These theoretical studies stress the importance of plasma drift in trough formation. In particular, horizontal velocities inside and outside the trough may give a good representation of how convection patterns are influencing the formation and shape of a trough. For example, rapid ion convection due to electric fields increases the ion temperature T_i by ion-neutral friction, which increases recombination rates and in turn lowers the electron density [Schunk and Sojka, 1982; Standley and Williams, 1984; Torr and Torr, 1979]. In addition, the competing rotation of the earth and the westward plasma convection produce a stagnation region in which the trough forms. The depleted plasma tubes formed in the nightside convect westward to the afternoon sector where they produce the pre-dusk troughs [Spiro et al., 1978].

This report further investigates the characteristics of the main trough using data from the Air Force Phillips Laboratories' high-latitude Digisonde network of [Buchau et al., 1988], Goose Bay (53.3N, 299.2E) and Argentina (47.3N, 306.0E), and the University of Massachusetts Lowell Digisonde at Millstone Hill (42.6N, 288.5E). Data for a six month period (January - June 1990) are analyzed and the statistical results are interpreted in terms of the theories on trough formation. The analysis concentrates on the dusk sector and the drift velocities involved in producing a stagnation region. Also the first occurrence in time of a trough detected at these stations is shown and comparisons to varying magnetic activity are discussed.

2.0 DIGISONDE DATA AND ANALYSIS METHOD

A network of digital ionosondes was used to collect the data. The Digisondes 256 sounders [Reinisch et al., 1989], unlike conventional ionosondes can operate as monitoring ionosondes (ionogram mode) for the routine recording of multi-parameter ionograms, and as an HF radar drift mode to measure the drift. In ionogram mode, the Digisonde reveals the ionograms and scales them in real time, providing all of the important ionospheric characteristics and the vertical electron density profiles [Reinisch and Huang, 1983]. In drift mode, the signals from each of the seven (or sometimes four) receiving antennas are Fourier transformed individually and digital beam forming is done for each Doppler component, thus separating the signals in the Doppler domain. Since in general, each reflected wave has a different Doppler shift due to the horizontal component of the ionospheric drift, echoes arriving in the same range bin are separated and identified. Then from the distribution of the Doppler sources the bulk velocity of the ionospheric plasma is derived [Reinisch et al., 1987; Cannon et al., 1991]. This line-of-sight HF Doppler technique measures the velocity of ionospheric irregularities, which we assume to be equal to the plasma bulk velocity.

Combining data from the two modes in the analysis it is possible to identify troughs from the variations of the critical frequency f_oF_2 and the peak height h_mF_2 of the F-layer, and to explain the trough formation with the help of the measured drift velocities. The ability of supplying ionospheric profiles as well as velocities makes the Digisonde a powerful tool in the investigation of ionospheric phenomena.

To detect the presence of the main trough at a particular station we analyzed the data in the following way: For the three most magnetically quiet days (lowest ΣKp) of each month the foF2 and hmF2 values were averaged to establish the "normal" diurnal behavior at each station. The comparison of the diurnal variation of each day with the quiet day average easily identifies the troughs. As an example, Figure 1 displays the diurnal variation of foF2, hmF2, and the horizontal and vertical velocity components observed at Millstone Hill on 25 January 1990. Universal time (UT = LT + 5h) is displayed on the horizontal axis at the bottom of the plot. The velocity plots use corrected geomagnetic coordinates. The vertical drift component V_z , shown on the top of the figure, varies from +50 to -50 m/s. The error bars represent one standard deviation away from the mean, determined for a measurement ensemble of approximately 100 samples. The second plot, labelled V_h , displays the horizontal velocity component as a vector which always begins on the central line. The directions are given on the right side by the N(orth), S(outh), E(ast) and W(est) characters. The magnitude of the vectors is specified by the 300 m/s scaling vector given on the left side of the figure.

The third panel displays the monthly quiet day average (labelled 'Q') and the current foF2 values in MHz. The quiet day average begins at ≈ 8 MHz at 00 UT while the January 25 curve begins at ≈ 6 MHz. The two curves are similar between 12 and 16 UT (07 to 11 LT), but after 16 UT the quiet day average is usually lower until 24 UT. A similar plot is shown for hmF2 at the bottom of Figure 1. The quiet day average begins around 210 km at 00 UT reaching a peak value of ≈ 250 km at around 06 UT, and after 12 UT levels off around 200 - 220 km. The daily variation in the peak height hmF2 for 25 January, however has a value of 300 km at 00 UT reaching a peak value of 380 km at ≈ 03 UT, and then it falls to a value of 210 km at 08 UT. The rise and fall of the peak of the layer tends to follow the change in vertical velocities observed at these times. The characteristic signature of a trough onset is clearly seen in Figure 1 as a decrease to low values of foF2, and an increase to high values of hmF2. The horizontal velocities show large westward drifts around 03 UT when the trough is observed.

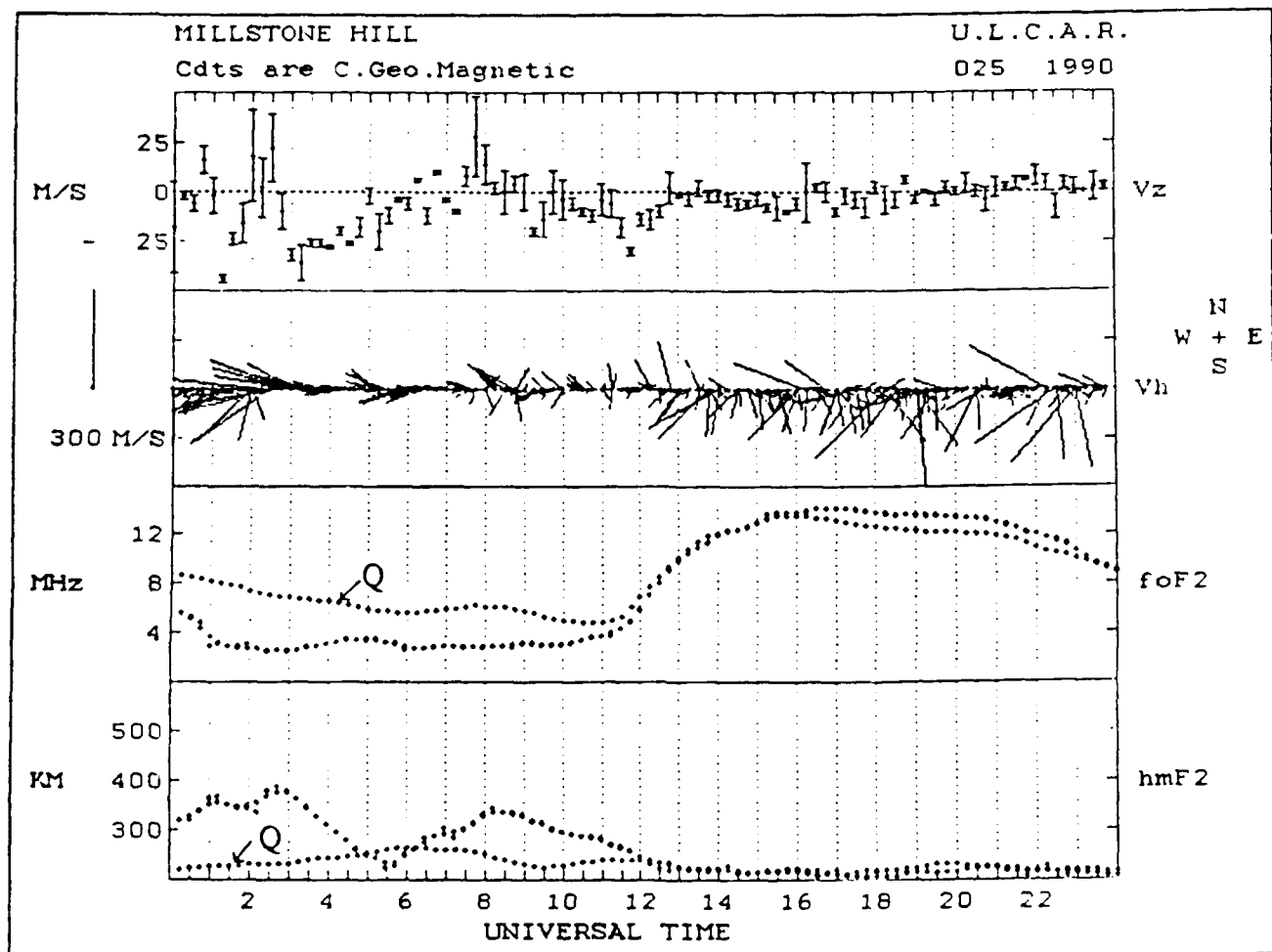


Figure 1. The diurnal variation of V_z , V_h , $foF2$ and $hmF2$ observed at Millstone Hill on 25 January 1991.

Defining the three quiet days average as the normal diurnal variation of the ionosphere appears to be a good standard to take. For example, Figure 2 displays the average quiet day variations of foF2 and hmF2 for the months of January, February, and March 1990 for the three stations Millstone Hill, Argentia and Goose Bay. In spite of the latitude and longitude separation of the stations the normal diurnal variations of foF2 and to some extent hmF2 are very similar, at least in January and February. For the month of March, however, the diurnal variations in foF2 and hmF2 for Goose Bay vary significantly from those observed at Argentia and Millstone Hill. In March 1990 the overall average ΣKp was $\approx 32+$, while for January and February the average ΣKp was $\approx 23+$. Clearly the trough had reached Goose Bay in March even during the three most quiet days, lowering foF2 during the day and producing low foF2 and high hmF2 values at night.

3.0 SYSTEMATIC TROUGH DETECTION

To investigate the occurrences of troughs at each station for each month, it is convenient to represent the differences between daily and normal variations in foF2 and hmF2 in terms of ratios. A "trough detection ratio" was defined which quickly allowed troughs to be identified in a large data set. This ratio may be defined as:

$$P_{hf} = p_{hmF2} / p_{foF2}$$

where:

$$\begin{aligned} p_{hmF2} &= (\text{hmF2 observed}) / (\text{3-quiet day average of hmF2}) \\ p_{foF2} &= (\text{foF2 observed}) / (\text{3-quiet day average of foF2}) \end{aligned}$$

From Figure 1 generally p_{foF2} is smaller than 1 and p_{hmF2} is greater than 1, which implies that P_{hf} is much larger than 1 when a trough is present. Applying this technique to a monthly data base conveniently reveals the occurrence of a trough. As an illustration Figures 3, 4 and 5 display contour plots of P_{hf} for the three stations in March. The Millstone Hill data (Figure 3) clearly indicate troughs on days 071 to 073 starting around 22 UT. An even more "pronounced" trough is observed on day 080 starting around 01 UT, resulting from an 82% reduction in electron density and a doubling in the peak height of the layer as compared to these

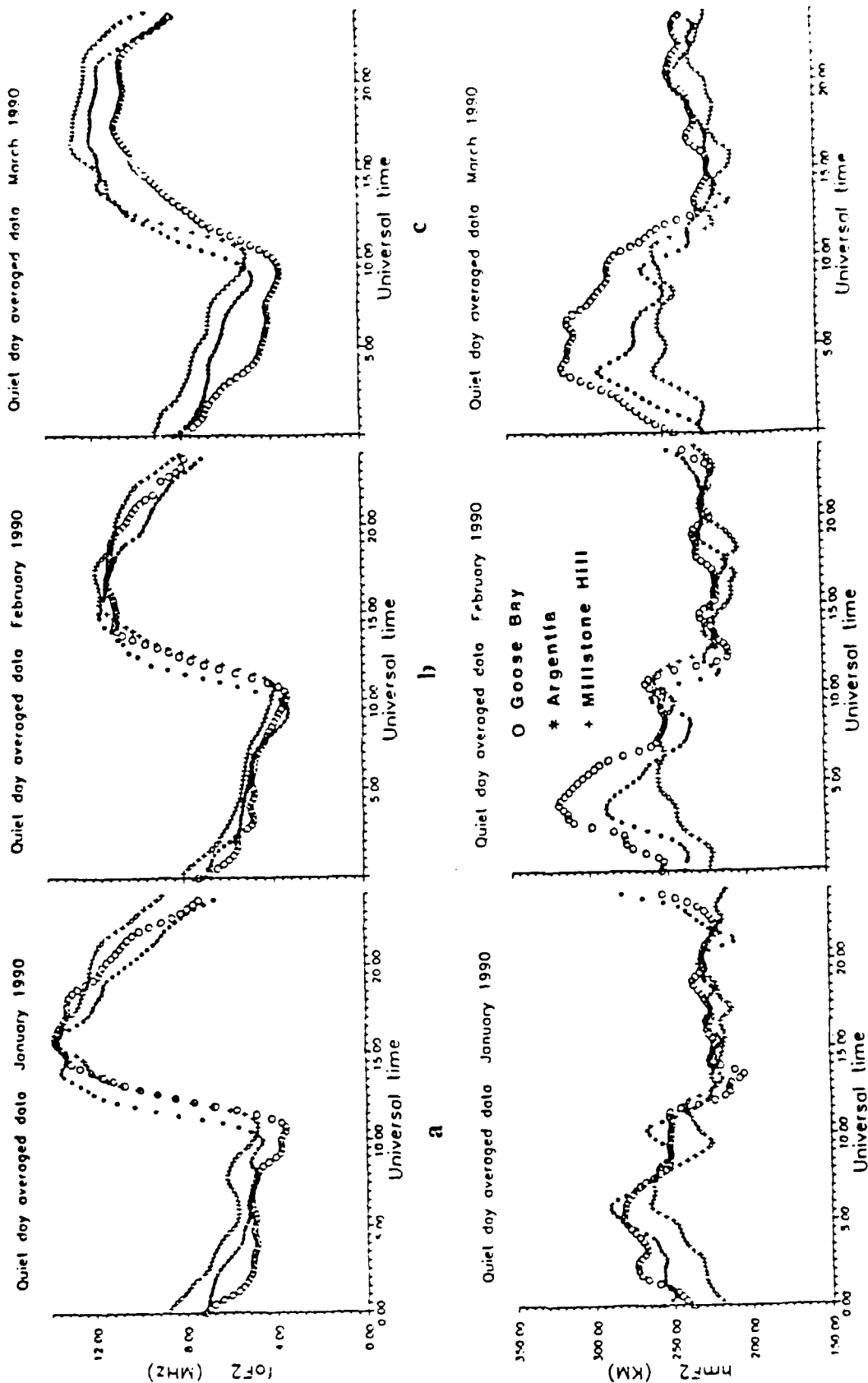


Figure 2. Diurnal variations in f_oF_2 (above) and h_mF_2 (below) averaged over the three most geomagnetically quiet days during the months of (a) January, (b) February and (c) March 1990.

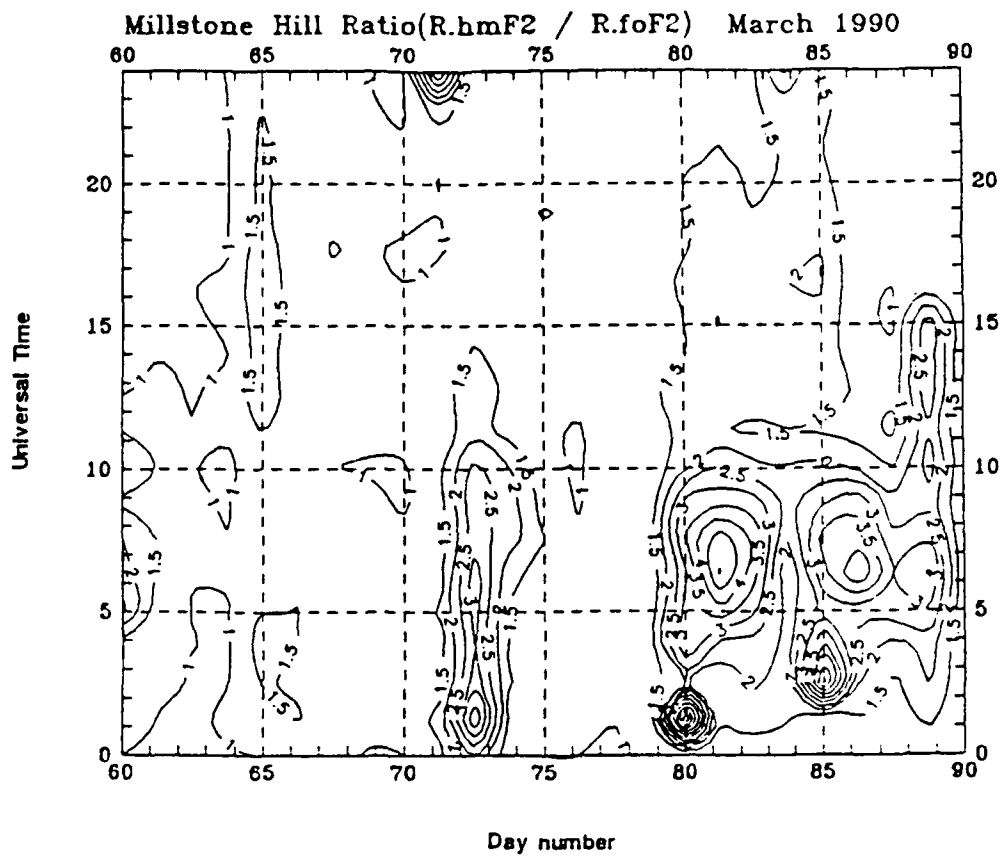


Figure 3. Contour plots for P_{hf} for March 1990 at Millstone Hill.

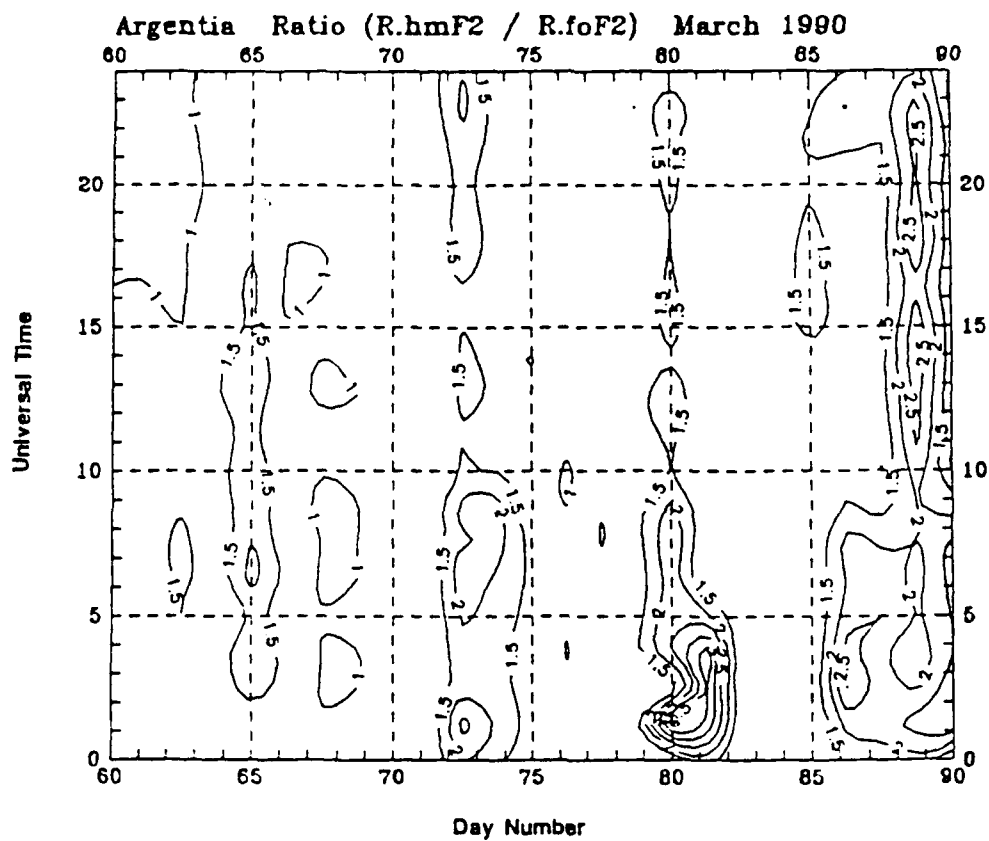


Figure 4. Contour plots for P_{hf} for March 1990 at Argentina.

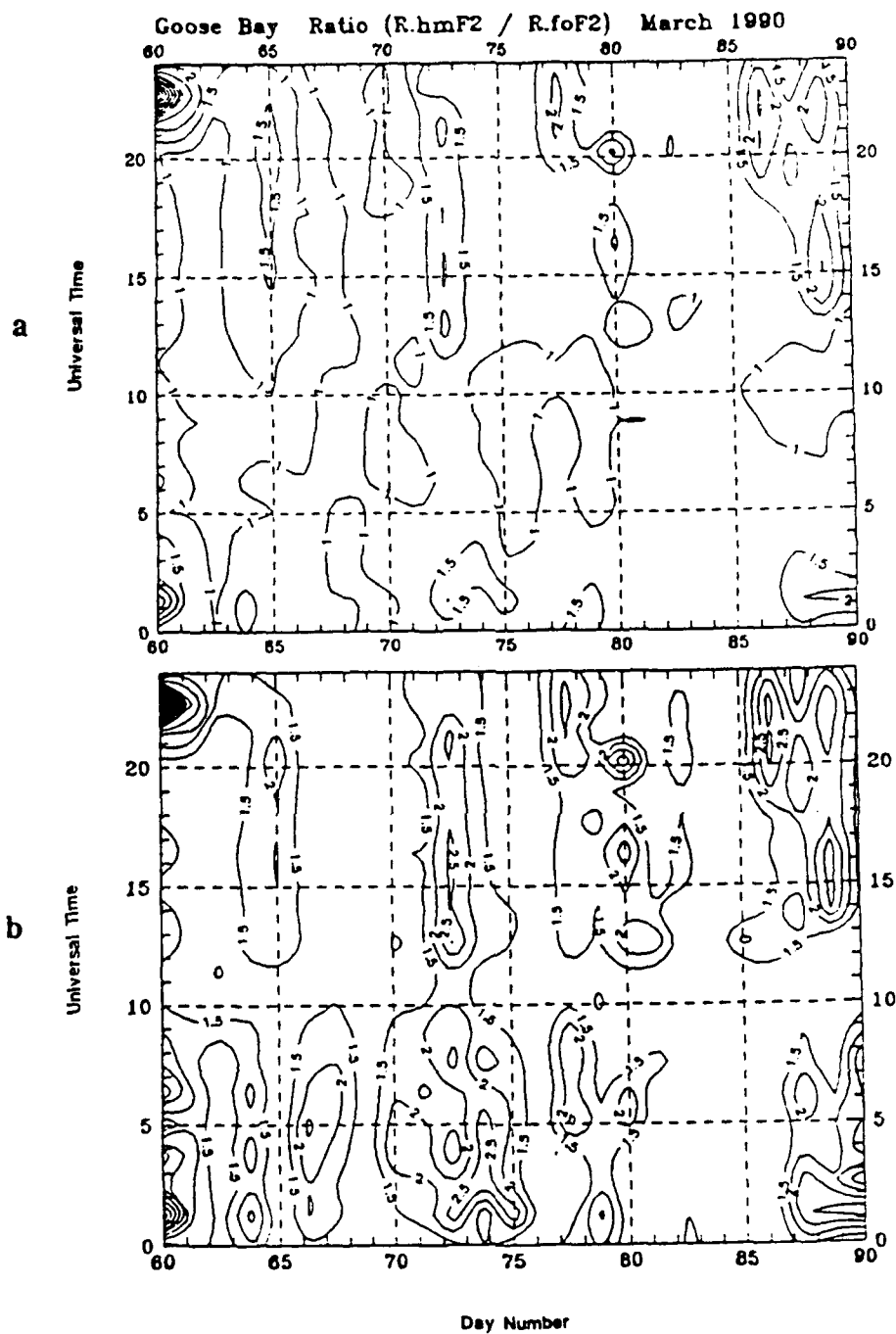


Figure 5. Contour plots for P_{hf} for March 1990 at Goose Bay. (a) Contours calculated using the 3-day average quiet days results recorded at Goose Bay, (b) Contours calculated using the 3-day average quiet days results recorded at Millstone Hill.

on quiet days. For day 080, the ΣKp was the highest for the month with a value of 46. After this day, troughs are consistently observed right up until day 089, where the last trough for this sequence of days is observed to begin at 04 UT.

Similarly contour plots for Argentina and Goose Bay are shown in Figures 4 and 5. The Argentina plots in Figure 4 are somewhat handicapped by lack of data for days 71, 72, 81 and 85. Troughs identified on days 073, 080, 086 to 089 display similar behavior to those observed at Millstone Hill, and the most extensive trough is again observed around day 080. The Goose Bay contours for P_{hf} (Figure 5a) are considerably different from the Millstone Hill and Argentina contours. Apart from the trough observed on day 060 at around 23 and 01 UT, no other large troughs are detected during this month. The detection of troughs at Goose Bay is not good using the P_{hf} method described above, since the first assumption made is that the average of the three most magnetically quiet days is taken as the normal diurnal variation in the ionospheric characteristics of this station. Yet as was observed in Figure 2, for March, the effects of the trough were already incorporated in the normal daily variations, since for the quiet days considered the ΣKp is on average 11 and the trough is located over Goose Bay. To illustrate the extent of the troughs located over Goose Bay P_{hf} was recalculated using the quiet day average recorded at Millstone Hill for March and the results are given in Figure 5b. From this figure it is clear that troughs are present over Goose Bay, however these troughs are not as pronounced as those detected at Millstone Hill and Argentina, and their times of occurrence are also different.

These contour plots were made for all six months and troughs identified. All in all, during the six month period from January to June 1990, 41 trough occurrences were identified at Millstone Hill, 44 at Argentina, and 55 at Goose Bay. Collecting the days where a trough was observed, it was possible to map the diurnal variation of the P_{hf} ratio with respect to ΣKp . For this analysis we assigned the values 0, 1, 2, 3 etc. to $Kp = 0, 0+, 1-, 1$, etc. and defined the sum SKp , so that $SKp = 3\Sigma Kp$.

In Figure 6, P_{hf} is plotted against SKp for all days when the trough was detected at Millstone Hill. It is immediately apparent that a lower limit exists in SKp below which troughs are not detected at Millstone Hill; this lower limit is SKp = 76, or an average of $K_p \approx 3$ in 3 hourly magnetic indices. For SKp = 76, troughs are first observed at 04 UT. As SKp increases the first detection of the trough is earlier, e.g. at SKp = 112 the trough is detected as early as 22 UT. Thus for a one unit increase in SKp the trough's occurrence is advanced by 10 minutes. The time variation itself is indicative of the trough moving to lower latitudes as K_p increases and being detected earlier at a particular station.

The analysis of 44 trough days at Argentia (Figure 7) shows a lower limit of SKp = 41 (or on average $\approx 1^+$) for trough occurrence at Argentia. Again with increasing SKp, trough occurrence at Argentia advances in time. For SKp = 45 a trough is detected at 02 UT, for SKp = 111 a trough is detected at 20 UT. Roughly, for each unit increase in SKp, the first trough occurs 5 minutes earlier. Again no movement to earlier times is observed when SKp increases beyond 126. The largest P_{hf} values are observed for SKp between 131 to 141. The extent of trough formation can also be observed from the troughs detected for SKp = 126. Both in Figures 6 and 7, troughs are evident well before 22 UT, usually still during daylight hours. While there is some significance placed on a value of SKp = 126, since in both Figures 6 and 7 it marks the stop of trough detection to earlier times, the troughs displayed in Figures 6 and 7 for this SKp value are all observed on the same day, i.e. 101 1990 (11 April 1990) and indicate that a large daytime trough existed which covered at least 5° of latitude and 18° of longitude.

Figure 8 displays P_{hf} plotted with respect to SKp for 55 days when troughs were detected at Goose Bay. For SKp = 21 (on average 0^+) troughs are detected at Goose Bay which indicates that on most occasions Goose Bay is located close to the main trough. The most pronounced troughs, displaying ratios as high as 3.2, occur at SKp = 73 and 100 at ≈ 22 UT. Unlike the lower latitude stations there is an upper limit to when troughs are no longer detected at Goose Bay, this being at SKp = 137. For values greater than this, the trough is always located equatorward of the station and Goose Bay observes ionospheric structure and convection patterns typical of an auroral or polar cap station.

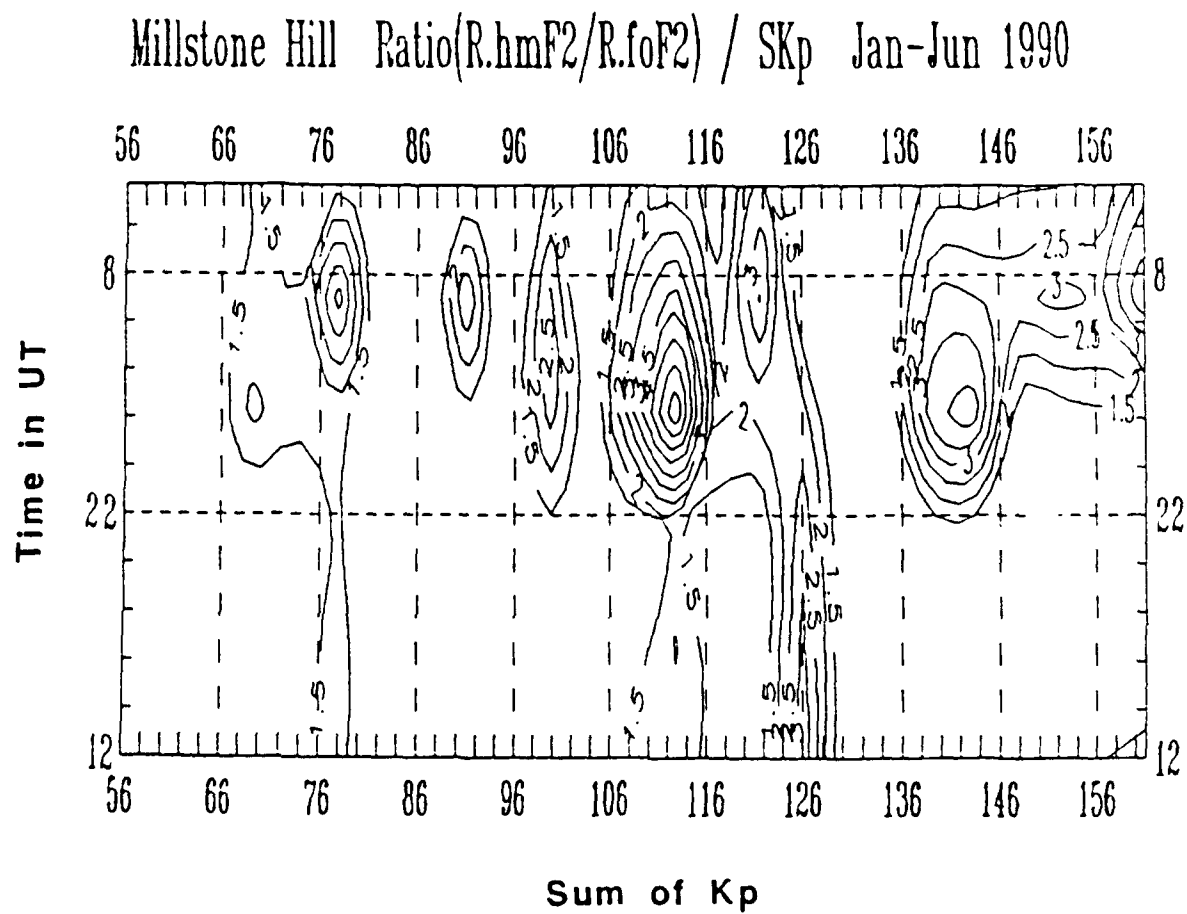


Figure 6. Ratio P_{hf} plotted with respect to sum of Kp for 41 days when troughs were detected at Millstone Hill.

Argentia Ratio(R_{hmF2}/R_{foF2}) / SKp Jan-Jun 1990

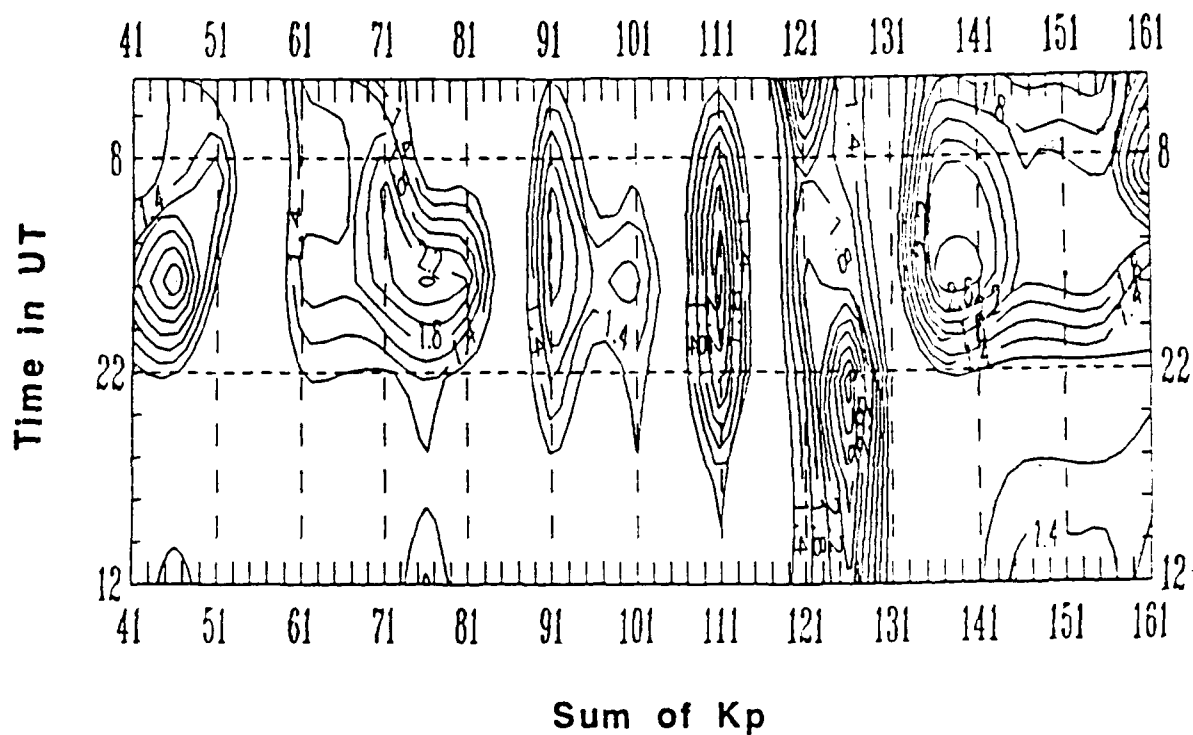


Figure 7. Ratio P_{hf} plotted with respect to sum of Kp for 44 days when troughs were detected at Argentia.

Goose Bay Ratio(R_{hmF2}/R_{foF2}) Jan-Jun 1990

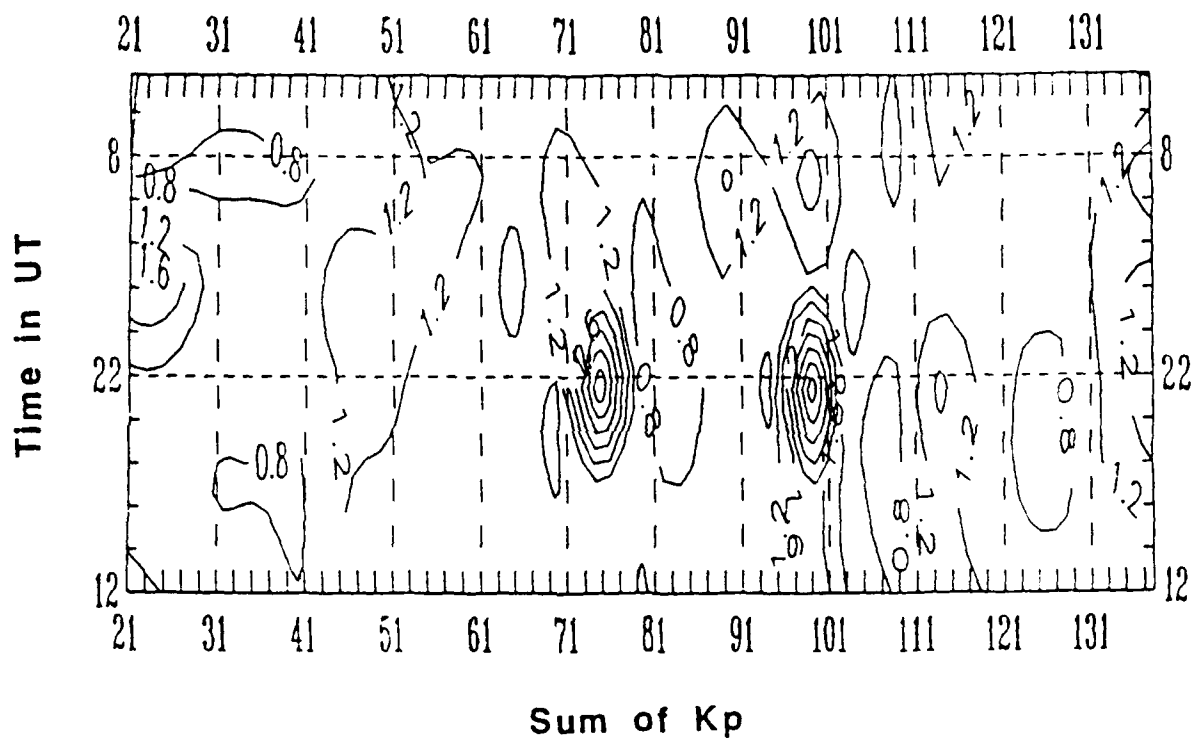


Figure 8. Ratio ρ_{hf} plotted with respect to sum of Kp for 55 days when troughs were detected at Goose Bay.

4.0 DRIFT VELOCITIES IN THE DUSK SECTOR

The two most promising theories used to explain the formation of the nocturnal trough are the so called stagnation and enhanced recombination theories. While both mechanisms are likely to be involved in the formation and maintenance of the main trough we have limited this investigation to the trough formation in the dusk sector where the stagnation theory has been shown through detailed calculations to work well [Sojka et al., 1981a, b]. Hence a discussion on the mechanism of the enhanced recombination theory will not be presented in this report.

The stagnation theory, first proposed by Knudsen [1974], takes into account the competing effects of the earth's rotation and the electric field induced convection [Knudsen et al., 1977; Spiro et al., 1978]. The theory states that flux tubes containing F-region plasma are convected from day to night across the polar cap with speeds typically in the order of 0.5–1.0 km/s. The motion is anti-sunward and upon reaching the nightside, the flux tubes containing the F-region plasma return to the dayside by drifting through the dawn and dusk sectors at lower latitudes. This so called two cell plasma flow and the effect of the earth's rotation results in the formation of a trough.

As an example Figure 9a shows the two cell convection pattern and the formation of a stagnation region by introducing co-rotation (Figure 9b) as calculated by Spiro et al. [1978]. Those flux tubes returning via the dusk sector must drift faster than the rotation of the earth in order to reenter the dayside. The opposing motion of westward drift and eastward rotation creates a stagnation region where the plasma confined in this region begins to decay via normal recombination processes within these flux tubes. The increased time in which electron density is depleted forms the trough at around 2200 CGLT (Figure 9b). Therefore one expects large westward velocities in this stagnation region in order for a trough to form, and this is typically what the Digisonde observations show.

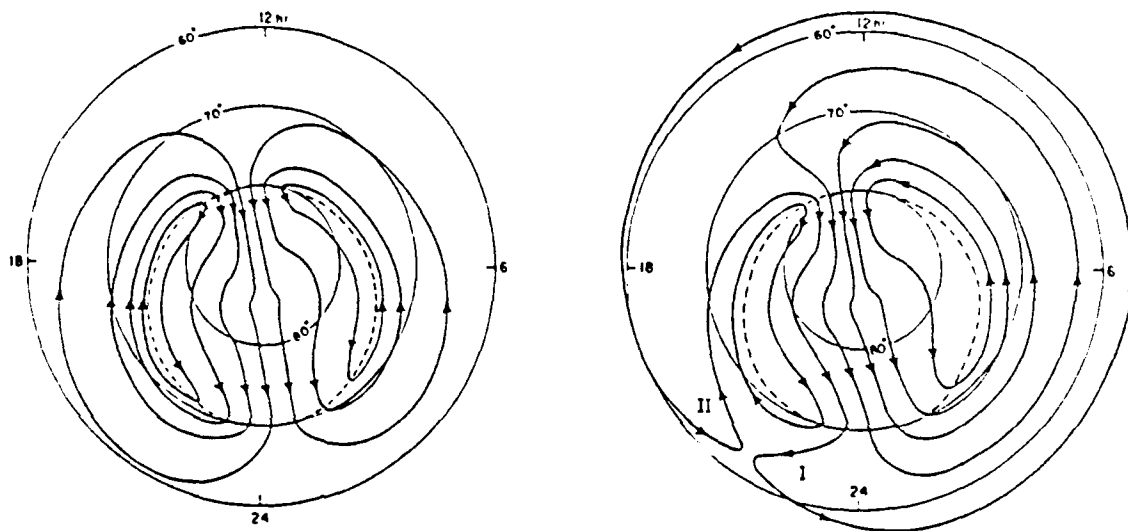


Figure 9. High latitude two cell convection pattern. (a) Represents the non rotating frame of reference while (b) corotation has been added. The flow stagnation point is located around 22 CGLT. Reproduced from Spiro et. al., [1978].

As an example we show the data in polar plots for day 047 1990 at Millstone Hill. On this day the main trough is first detected at approximately 19 CGLT, as indicated by the characteristic drop in foF2 (Figure 10a) and an increase in hmF2 (Figure 10b). The horizontal velocity component V_h (Figure 10c) dramatically increases in magnitude during this time pointing in a SW direction opposing the rotation of the earth; V_h reaches a maximum value of ≈ 550 m/s. (a reference scale of 340 m/s is given on the right of the plot). A second height rise observed at ≈ 01 CGLT is associated with large V_h vectors of ≈ 340 m/s. Thereafter the horizontal speed decreases to ≈ 115 m/s. After 06 CGLT (around F-region sunrise) the vertical velocities (Figure 10d) are consistently negative while the horizontal velocity component flips to a SE direction. This eastward flow is maintained until 15 CGLT when the V_h vector again flips to the westward direction. The change from westward to eastward convection at dawn is consistently observed at Millstone Hill for quiet times, as long as the main trough remains poleward of the station. However for higher SKp values (usually > 120) the flip over of the V_h vector from westerly to easterly drifts occurs earlier and the general drift pattern compares well with that of Figure 9a. Two good examples of this behavior are shown in Figure 11.

Figures 11a and b display the horizontal velocity vectors recorded at Millstone Hill over the two days 103 and 104 1990 respectively. Prior to these days a SKp of 150 was recorded. In Figure 11a (for day 103) the horizontal velocity vector V_h is displayed and the scale set to 200 m/s. At approximately 03 CGLT the vector flips from SW to the SE direction. At 09 CGLT the vector constantly points towards the NE until 14 CGLT when it flips back to NW then SW. The drift vectors outline a two cell convection pattern with a dayside cusp at 14 CGLT and nightside discontinuity at 02 CGLT similar to the convection pattern shown in Figure 9a for a non-rotating frame of reference. Similarly, Figure 11b shows the same behavior for day 104 where the dayside cusp is at 15 CGLT and the nightside discontinuity at 02 CGLT. All vectors follow a two cell convection pattern.

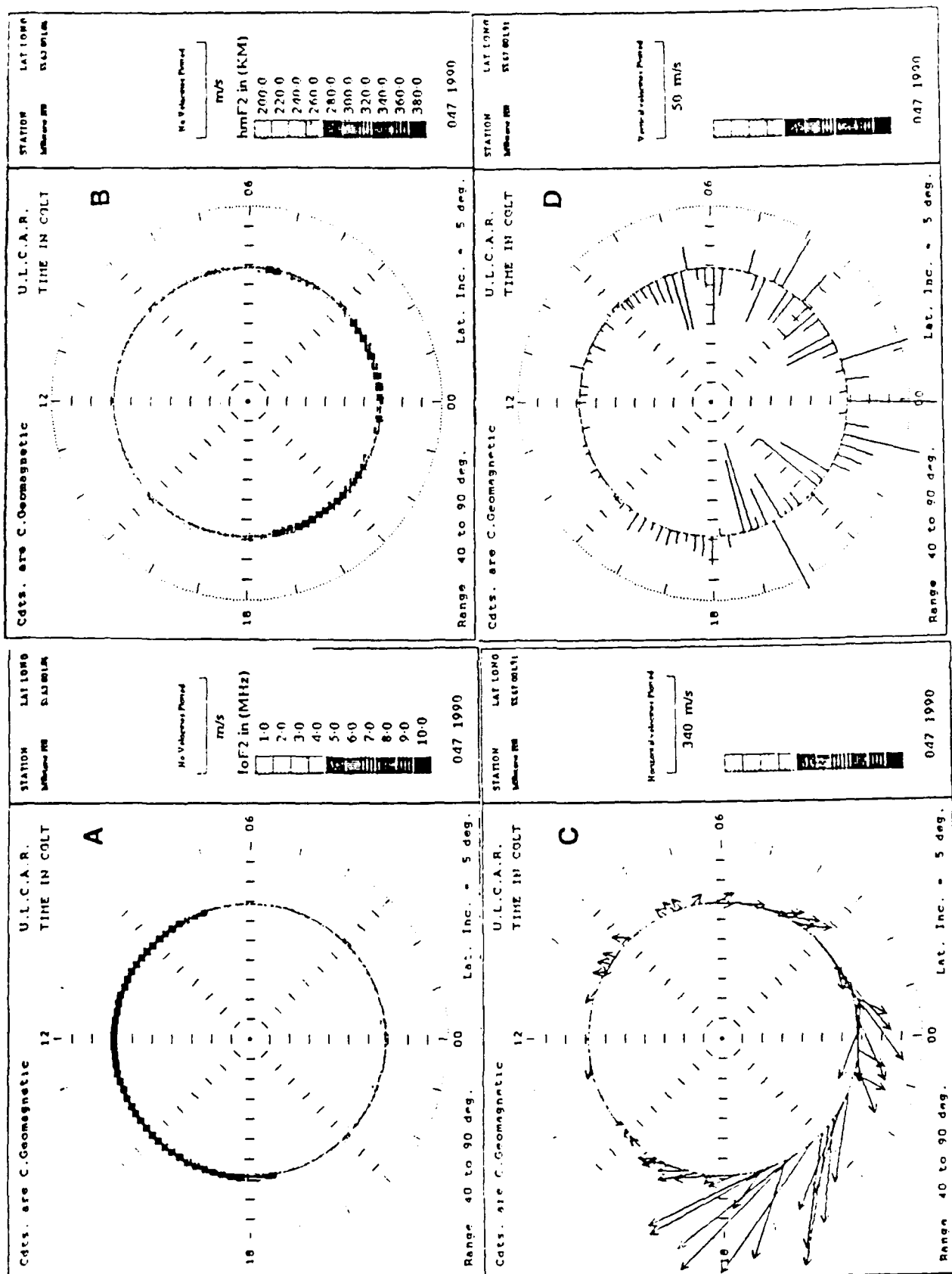


Figure 10. Polar plots for (1) foF2, (b) hmF2, (c) Vh and (d) Vz, observed at Millstone Hill on day 047 1990.

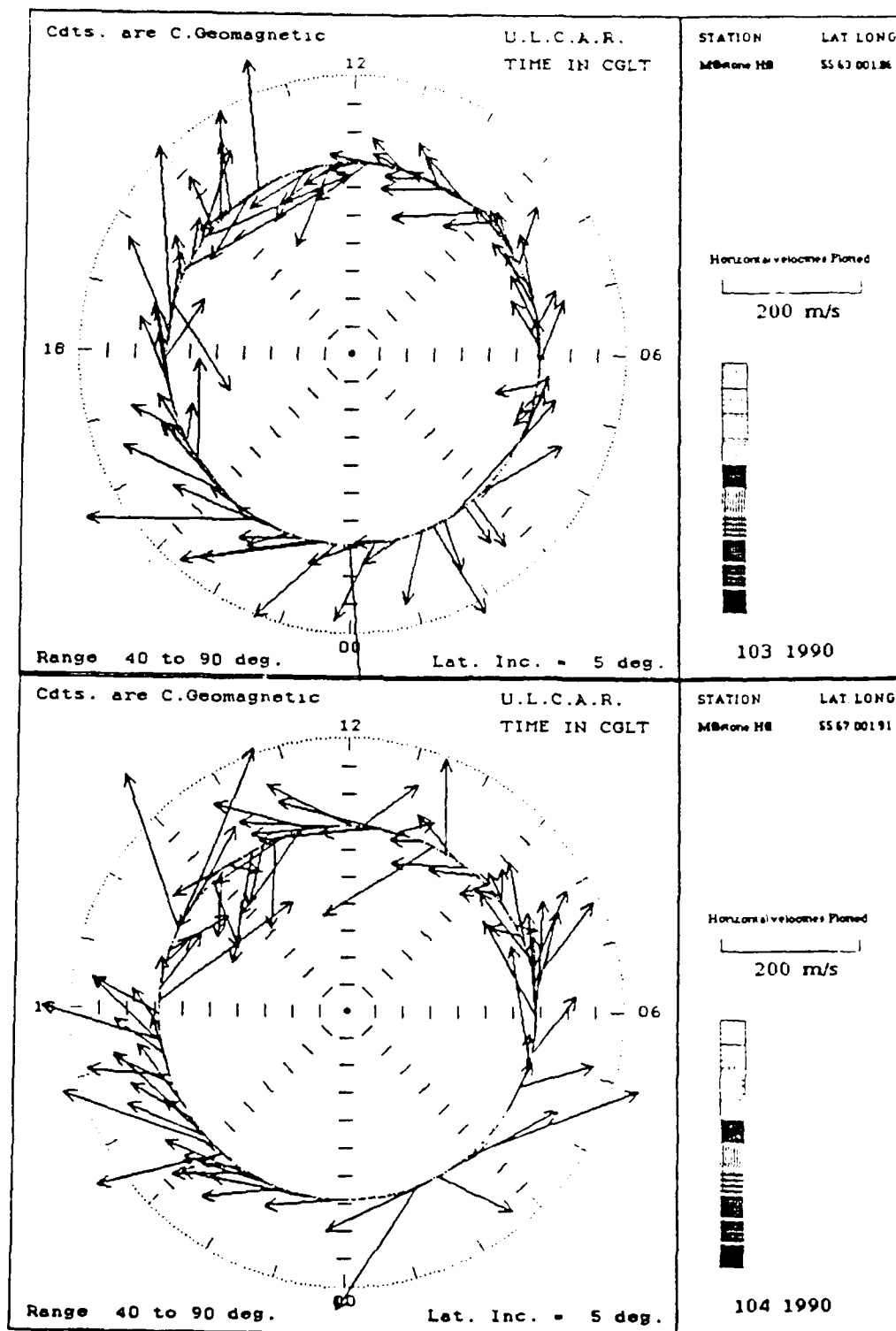


Figure 11. Polar plot of horizontal velocity vectors observed at Millstone Hill on days (a) 103 and (b) 104, 1990.

The effects of a large westward drift on the formation of troughs can also be seen at the other stations. Figure 12 shows a trough observed at Argentia on day 38 1990. The horizontal drift velocity V_h (Figure 12c) begins to increase at around 16 CGLT reaching a maximum value of 450 m/s at 20 CGLT. In comparison foF2 reaches its lowest value at ≈ 20 CGLT where the peak height of the layer is at 280 km. After this time the velocities decrease and the peak of the layer hmF2 falls back to 200–220 km while foF2 increases to 7.0 MHz. During 18–20 CGLT the vertical velocity was negative. The observed downward motion explains why the layer peak in the trough did not reach greater heights than 280 km, as is usually observed.

Figure 13 shows a trough observed at Goose Bay on day 138, 1990. Again the largest velocity vectors for V_h at values of ≈ 514 m/s are observed from 16 to 20 CGLT. The layer peak height hmF2 reaches values above 360 km between 18 to 20 CGLT and during this time foF2 falls from 6 to 4 MHz. The horizontal velocity drift (Figure 13c) vectors outline again a two cell convection pattern much as was observed in Figure 11. In this case the dayside cusp is located at ≈ 14 CGLT and the nightside discontinuity is at ≈ 01 CGLT. The magnitude of the westward drift in the dusk sector need not always be as large or greater than the rotation velocity of the earth as long as it is large enough to slow the motion of plasma into the nightside and lengthen the time over which normal recombination processes deplete the ionization. Taking into account all the trough cases recorded, plots of the average drift velocities are produced.

Figure 14 shows the drifts parameters calculated from 41 days in which troughs were detected at Millstone Hill. The magnitudes of the horizontal and vertical velocities were sampled for each day and the mean of the distributions plotted with respect to CGLT. For the azimuth angles the medians were used since the mean may not properly handle the 0–360° transition. The results in Figure 14 show the points plotted and a 10 point polynomial line of best fit used. In Figure 14a it is clear that the azimuth of the horizontal velocity component shifts from west at 00 CGLT to south at ≈ 06 CGLT, to east at 12 CGLT, to south at 18 CGLT, and back to west at 23 CGLT.

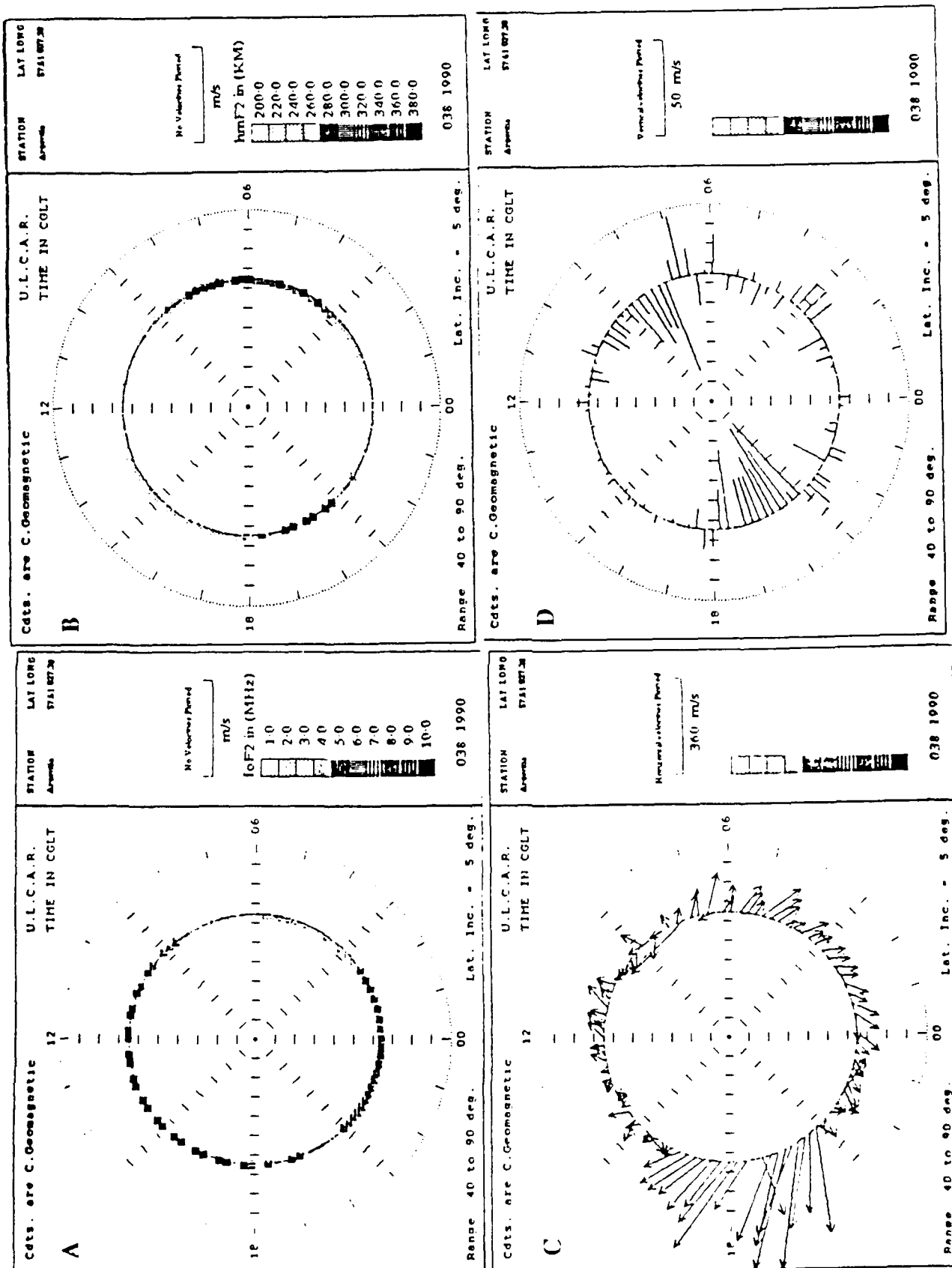


Figure 12. Polar plots for (a) foF2, (b) hmF2, (c) Vh and (d) Vz, observed at Argentina on day 38, 1990.

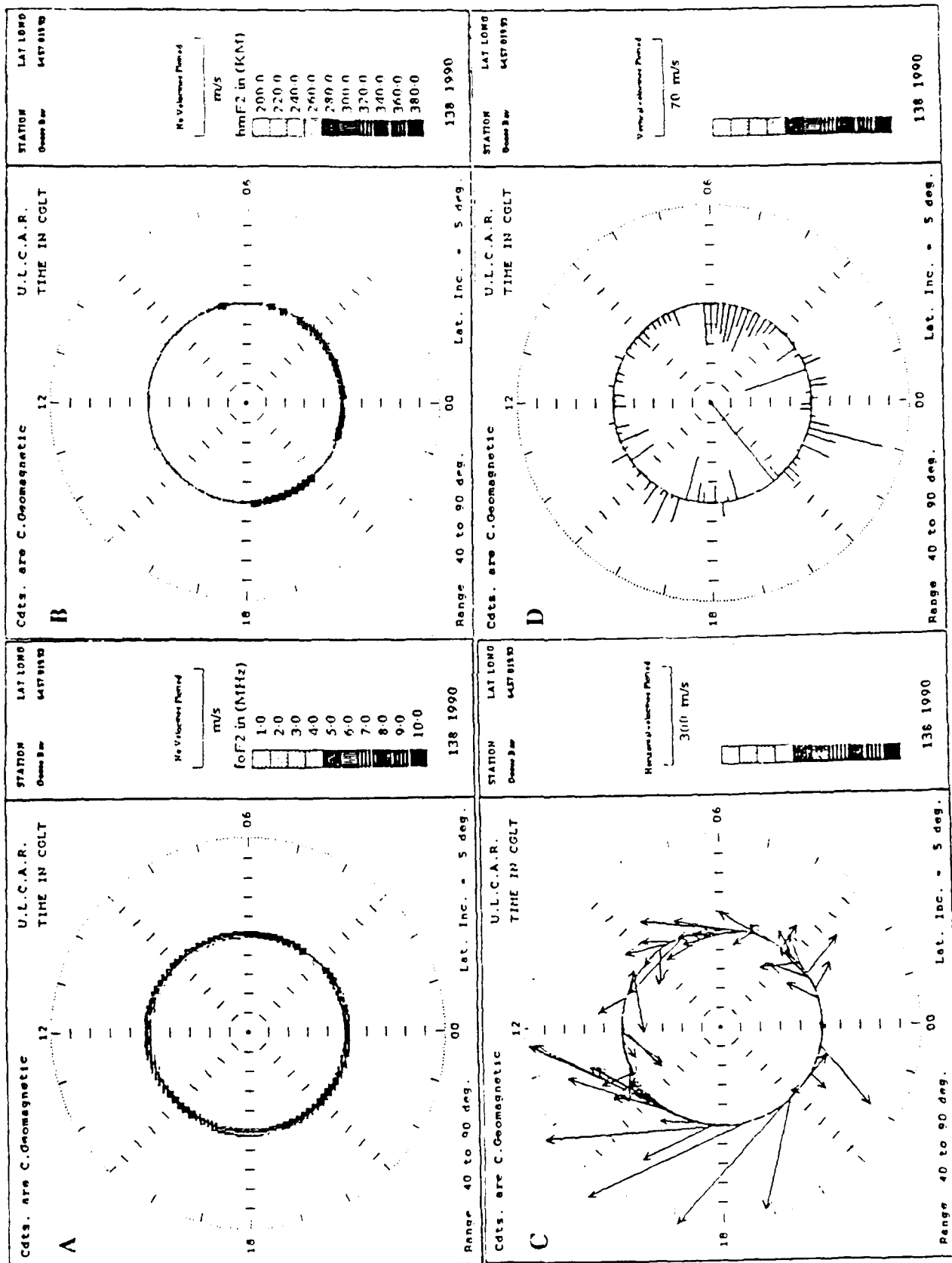


Figure 13. Polar plots for (a) foF2, (b) hmF2, (c) Vh and (d) Vz, observed at Goose Bay on day 138, 1990.

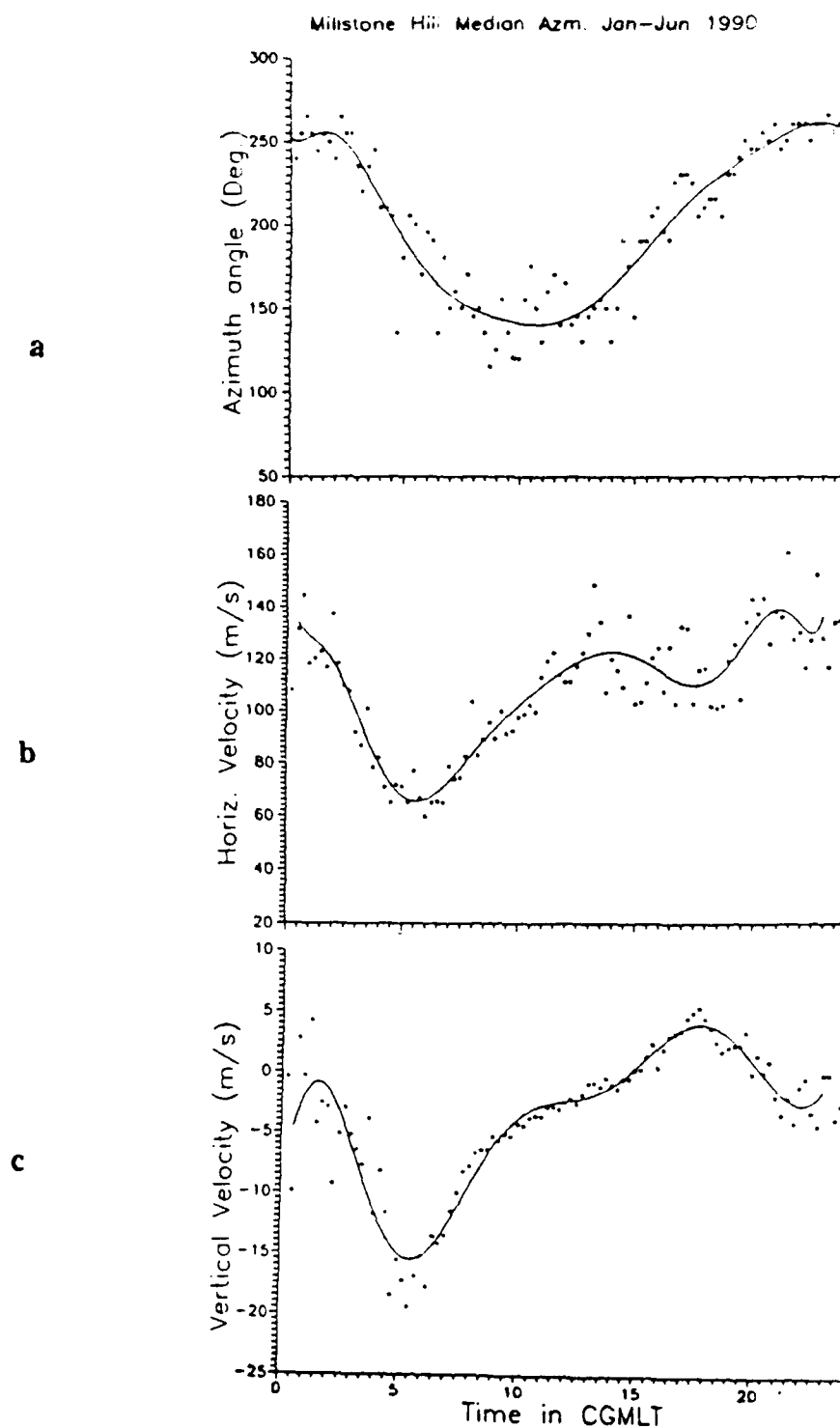


Figure 14. Statistical analysis of Az, Vh and Vz measured over 41 days when troughs were detected at Millstone Hill during January - June, 1990, (a) median of Az, (b) mean of $|V_h|$ and (c) mean of $|V_z|$.

Figure 14b displays the magnitude of the horizontal component V_h . The marked drop at 06 CGLT to ≈ 65 m/s in the horizontal velocity corresponds to F-region sunrise, when the velocity vector is changing its azimuth angle from a SW to SE direction. The magnitude then increases and reaches a maximum of ≈ 140 m/s at around 21 CGLT, which is not surprising in light of the discussions on trough formation in the dusk sector, where we expect the velocity magnitudes to be large depending upon the value of ΣK_p . Note that the data base considered was limited to 41 days when troughs were detected. As we have shown in Figures 6 and 7, the first occurrence of trough changes with ΣK_p , which is a result of the expansion or contraction of the two cell convection pattern. Hence the mean of the velocity vector represents the overall average, which means that depending on trough position the station may not always be located under the stagnation point but may cross the trough boundaries at later or earlier times. As a result the mean magnitude of the horizontal component is nowhere as dramatic as observed in the individual cases shown in Figures 11, 13 and 14. The mean vertical drift component has a sharp drop to ≈ -15 m/s around 05 CGLT, after which it decreases to zero at around 15 CGLT. The vertical velocity is positive reaching a peak value of 4 m/s at 18 CGLT and then falls through zero to negative velocities.

Figure 15 shows the statistical drift parameters calculated from 44 days in which troughs were detected at Argentina, while Figure 16 shows results calculated from 55 days in which troughs were detected at Goose Bay. In comparing Figures 14, 15 and 16, it is clear that the largest mean horizontal velocity occurs around 21 CGLT when drift is in a SW direction. The statistical results presented here indicate that the magnitude and orientation of the horizontal velocities at around 21 CGLT are consistent with the requirements for the formation of a stagnation region. It is interesting also to note that a gradient in the vertical velocities exists as latitude increases. For example, Millstone Hill displays general negative vertical velocities, while Argentina displays velocities around zero and Goose Bay has vertical velocities that are generally positive. Note that the statistical variation in A_z , V_h , V_z presented in this report reflect the average of convection patterns which exist when troughs are present and by no means should be inferred to the general behavior of the ionosphere over each station during geomagnetically quiet times.

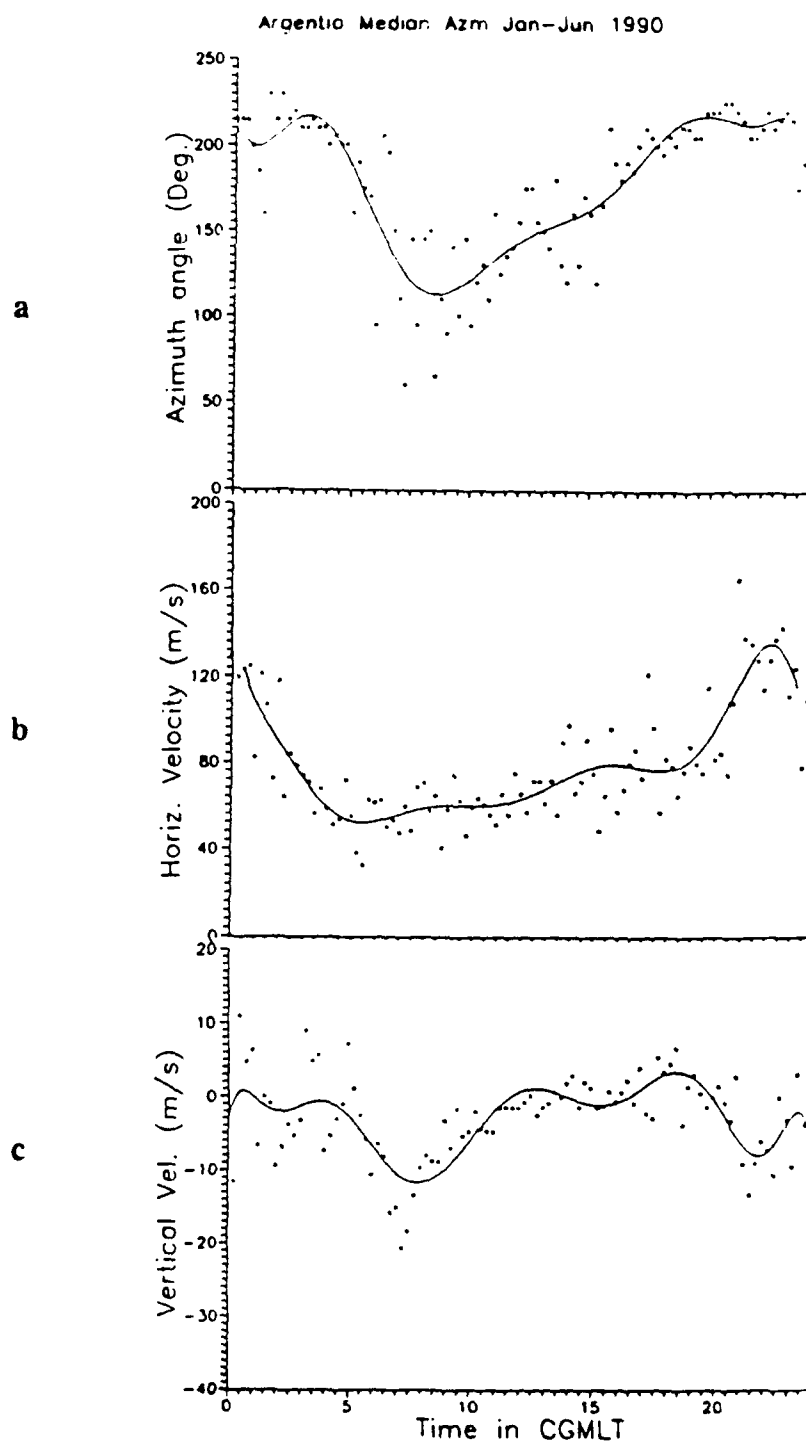


Figure 15. Statistical analysis of Az, Vh and Vz measured over 44 days when troughs were detected at Argentia during January - June, 1990, (a) median of Az, (b) mean of $|V_h|$ and (c) mean of $|V_z|$.

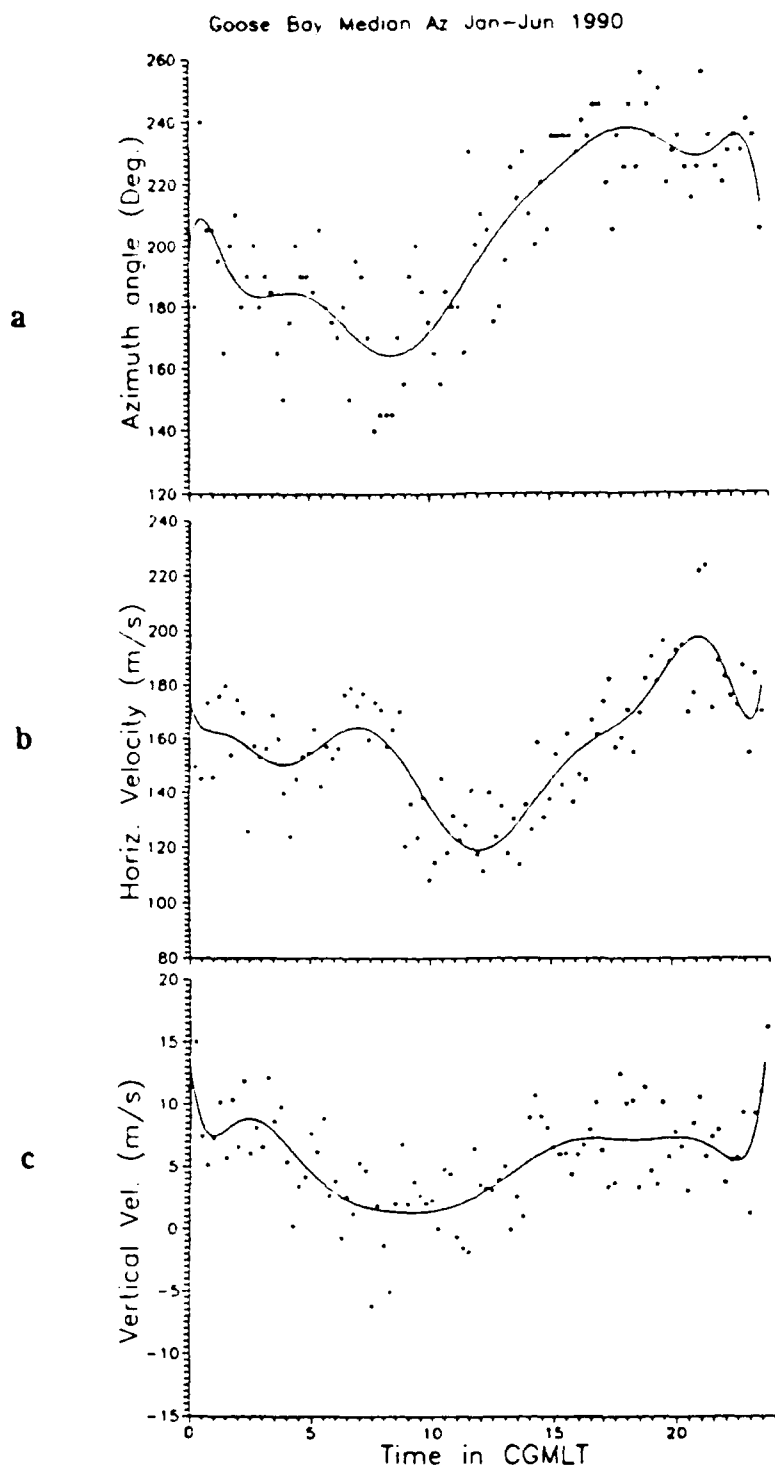


Figure 16. Statistical analysis of Az, Vh and Vz measured over 55 days when troughs were detected at Goose Bay during January - June, 1990, (a) median of Az, (b) mean of $|V_h|$ and (c) mean of $|V_z|$.

5.0 CONCLUSION

The characteristics of the main trough observed at Goose Bay, Argentina and Millstone Hill for the period from January-June 1990 were investigated. The results indicate:

1. The three (magnetic quiet) day average used in the analysis is a good standard to take in describing the normal diurnal variation at a station. Comparisons between foF2 and hmF2 diurnal variations observed at the three stations indicate that as long as the overall ΣKp for the month is low, the behavior of the ionosphere at each station is very similar.

2. As ΣKp increases, the first detection of a trough at Millstone Hill and Argentina is recorded earlier in the night. Generally for a one unit increase in ΣKp the trough is detected 10 minutes earlier at Millstone Hill and 5 minutes earlier at Argentina. A trough can be detected at Millstone Hill generally when $\Sigma Kp > 76$, usually after 04 CGLT, at Argentina when $\Sigma Kp > 45$ after 02 CGLT, and at Goose Bay when $\Sigma Kp > 21$.

3. The Digisonde observations clearly show large westward drifts in the troughs. The orientation and magnitude of the horizontal component of drift opposes the eastward rotation of the earth as expected from a stagnation point theory. For higher ΣKp when the trough is located equatorward of the stations the measured drifts outline a two cell convection pattern. The dominant mechanism for the trough formation seems to be the interaction of the magnetospherically driven polar convection pattern in the dusk sector and the eastward co-rotation, i.e. stagnation mechanism modeled by Spiro et al. [1978]. Statistical analysis of all the days in which troughs were detected also indicate that the largest velocity magnitudes are recorded around 22 CGLT when the horizontal velocity drift component is oriented to the west.

6.0 REFERENCES

Banks, P.M., R.W. Schunk and W.J. Raitt, "NO⁺ and O⁺ in the High Latitude F-Region," *Geophys. Res. Lett.*, Vol. 1, pp. 239-242, 1974.

Buchau, J., B.W. Reinisch, D.N. Anderson, E.J. Weber and C. Dozois, "Polar Cap Plasma Convection Measurements and Their Relevance to the Modeling of the High-latitude Ionosphere," *Radio Sci.* pp 23, 521, 1988.

Cannon, P.S., B.W. Reinisch, J. Buchau and T. Bullett, "Response of the Polar Cap F-Region Convection Direction to Changes in the Interplanetary Magnetic Field: Digisonde Measurements Northern Greenland," *J. Geophys. Res.*, Vol. 96, pp. 1239-1250.

Evans, J.V., J.M. Holt, W.L. Oliver and R.H. Wand, "The Fossil Theory of Nighttime High Latitude F-Region Troughs," *J. Geophys. Res.*, Vol. 88, pp. 7769-7782, 1983.

Halcrow, B.W. and J.S. Nisbet, "A Model of F2 Peak Electron Densities in the Main Trough Region of the Ionosphere," *Radio Science*, Vol. 12, pp. 815-820, 1977.

Knudsen, W.C., "Magnetospheric Convection and the High-Latitudes F2 Ionosphere," *J. Geophys. Res.*, Vol. 79, pp. 1046-1955, 1974.

Knudsen, W.C., P.M. Banks, J.D. Winningham, and D.M. Klumpar, "Numerical Model of the Convecting F2 Ionosphere at High Latitudes," *J. Geophys. Res.*, Vol. 82, pp. 4784-4792, 1977.

Liszka, L. and T. Turunen, "On the Relation Between Auroral Particle Precipitation and the Ionospheric Trough," *Kiruna Geophysical Observatory, Preprint No. 70*, 1970.

Mendillo, M. and C.C. Chacko, "The Baseline Ionospheric Trough," *J. Geophys. Res.*, Vol. 82, pp. 5129-5137, 1977.

Muldrew, D.B., "F-Layer Ionization Troughs Deduced from Alouette Data," J. Geophys. Res., Vol. 70, pp. 2635-2650, 1965.

Reinisch, B.W. and X. Huang, "Automatic Calculations of Electron Density Profiles from Digital Ionograms, 3. Processing of Bottomside Ionograms," Radio Science, Vol. 18, p. 477, 1983.

Reinisch, B.W., J. Buchau and E.J. Weber, "Digital Ionosonde Observations of the Polar Cap F-Region Convection," Physica Scripta, Vol. 36, pp. 372-377, 1987.

Reinisch, B.W., K. Bibl, D.F. Kitrosser, G.S. Sales, J.S. Tang, Z.M. Zhang, T.W. Bullett, and J.A. Ralls, "The Digisonde 256 Ionospheric Sounder," World Ionosphere/Thermosphere Study WITS Handbook, Vol. 2, Ed. by C.H. Liu, December 1989.

Rycroft, M.J. and J. Burnell, "Statistical Analysis of Movements of the Ionospheric Trough and the Plasmapause," J. Geophys. Res., Vol. 75, pp. 5600-5604, 1970.

Rycroft, M.J. and J.O. Thomas, "The magnetospheric Plasmapause and the Electron Density Trough at Alouette I Orbit," Planet Space Sci., Vol. 18, pp. 65-80, 1970.

Schunk, R.W. and J.J. Sojka, "Ion Temperature Variations in the Dayside High-Latitude F-Region," J. Geophys. Res., Vol. 87, pp. 5169-5183, 1982.

Schunk, R.W., W.J. Raitt and P.M. Banks, "Effect of Electric Fields on the Daytime High-Latitude E and F-Regions," J. Geophys. Res., Vol. 80, pp. 3121-3130, 1975.

Sharp, G.W., "Mid-Latitude Trough in the Night Ionosphere," J. Geophys. Res., Vol. 71, pp. 1345-1356, 1966.

Sokja, J.J., W.J. Raitt and R.W. Schunk, "A Theoretical Study of the High-Latitude Winter F-Region at Solar Minimum for Low Magnetic Activity," J. Geophys. Res., Vol. 86, pp. 609-621, 1981a.

Sokja, J.J., W.J. Raitt and R.W. Schunk, "Plasma Density Features Associated with Strong Convection in the Winter High-Latitude F-Region," J. Geophys. Res., Vol. 86,

pp. 6968-6916, 1981b.

Spiro, R.W., R.A. Heelis and W.B. Hanson, "Ion Convection and the Formation of the Mid-Latitude F-Region Ionization Trough," J. Geophys. Res., Vol. 83, pp. 4255-4264, 1978.

Standley, P.J. and P.L.S. Williams, "The Maintenance of the Nighttime Ionosphere at Mid-Latitudes 1. The Ionosphere Above Malvern," J.A.T.P., Vol. 46, pp. 73, 1984.

Torr, M.R. and D.G. Torr, "Chemistry of the Thermosphere and Ionosphere," J.A.T.P., Vol. 41, pp. 73, 1984.

Watanabe, S., K-I. Oyama and T. Abe, "Electron Temperature Structure Around Mid-Latitude Ionospheric Trough," Planet, Space. Sci., Vol. 37, pp. 1453-1460, 1989.

Whalen, J.A., private communication, 1992.